Journal of Magnetism and Magnetic Materials 502 (2020) 166551

Contents lists available at ScienceDirect

Journal of Magnetism and Magnetic Materials

journal homepage: www.elsevier.com/locate/jmmm

Research articles

# Multiple transitions and wide refrigeration temperature range in $R_3NiSi_2$ (R = Tb, Dy) compounds

Jun Liu[a,b], Zhiyi Xu[c], Jiawang Xu[d], Shulan Zuo[a,b], Yan Zhang[a,b], Dan Liu[a,b], Xinqi Zheng[d], Lichen Wang[e], Tongyun Zhao[a], Fengxia Hu[a,b], Jirong Sun[a,b], Baogen Shen[a,b,*]

[a] State Key Laboratory of Magnetism, Institute of Physics, Chinese Academy of Sciences, Beijing 100190, People's Republic of China
[b] University of Chinese Academy of Sciences, Beijing 100049, People's Republic of China
[c] National Institute of Metrology, Beijing 100029, People's Republic of China
[d] School of Materials Science and Engineering, University of Science and Technology Beijing, Beijing 100083, People's Republic of China
[e] Technical Institute of Physics and Chemistry, Chinese Academy of Sciences, Beijing 100090, People's Republic of China

ARTICLE INFO

*Keywords:*
Magnetocaloric effect
Magnetic transitions
Magnetic refrigeration

ABSTRACT

In this work, orthorhombic polycrystalline $Tb_3NiSi_2$ and $Dy_3NiSi_2$ compounds were prepared and magnetocaloric effect during multiple magnetic transitions was investigated in detail. $Tb_3NiSi_2$ compound displays four different magnetic transitions at 94 K, 115 K, 134.2 K, and 140.6 K, respectively. The maximal value of magnetic entropy change are about 4.5 J/kg K and 11.1 J/kg K at 141 K for $Tb_3NiSi_2$ compound under a field change of 0–2 T and 0–7 T, respectively. For the $Dy_3NiSi_2$ compound, three obvious magnetic transitions are found at 29.3 K, 65.4 K, and 76.6 K and the maximal value of magnetocaloric effect are about 3.6 J/kg K and 10.8 J/kg K at 77 K for a field change of 0–2 T and 0–7 T, respectively. Due to the multiple magnetic transitions, both compounds exhibit the wide refrigeration temperature range and considerable refrigerant capacity. The results reveal that the value of refrigeration temperature range and refrigerant capacity are 66.9 K and 549.1 J/kg for $Tb_3NiSi_2$ compound, and 64.0 K and 489.6 J/kg for $Dy_3NiSi_2$ compound, respectively. Therefore, $R_3NiSi_2$-family compounds have a potential application in middle temperature magnetic refrigeration.

## 1. Introduction

The phenomenon producing the exothermic or endothermic heat for magnetic materials when the field is enhanced or weakened is known as magnetocaloric effect (MCE) [1]. Since the sheet-shaped Gd was firstly used as magnetic refrigerant [2], the exploration of magnetic refrigeration materials has been carried out and great progress has been made in the past decades. Large magnetic entropy change materials have always been the focus of researchers in the area of magnetic refrigeration because of their high energy efficiency and eco-friendly characteristics [3–5]. In general, magnetic refrigeration materials are classified into three categories in terms of temperature range. Those materials with low temperature range of refrigeration (below 80 K) such as $Gd_3(SO_4)_2{\cdot}8H_2O$ [6], $Gd_3Ga_5O_{12}$ [7,8], $Dy_3Al_5O_{12}$ [9], RFeSi [10,11], HoCoGe [12], and CeSi [13], and room temperature range of refrigeration (above 250 K) such as Gd [14,15], $Gd(Si, Ge)_4$ [16,17], $La(Fe,Si)_{13}$ [18–22], have widely been investigated. At the same time, Singh et al. [23] and Ćwik [24,25] carried out a detailed study for a series of multicomponent $RT_2$ (R = rare earth, T = transition metal) alloys with the intermediate temperature range of refrigeration. But comparatively speaking, magnetic entropy change materials in middle temperature range (between 80 K and 250 K) seem to get less attention since this temperature zone is in the range of liquid nitrogen temperature. However, it is an indispensable part for development of magnetic refrigeration materials in the future.

A kind of desired magnetic refrigeration material has not only the large magnetic entropy change but also the broad refrigeration temperature range ($\Delta T_{width}$) and the high refrigerant capacity (RC). According to the previous results [26–28], multiple magnetic transitions in materials can be used as an effective approach to enhance the value of $\Delta T_{width}$ and RC. Recently, the $La_3NiGe_2$-type $R_3TX_2$ alloys (R = rare-earth metal, T = transition metal, X = main group element) have been studied for many interesting magnetic properties [29–34]. Tencé et al. firstly reported the magnetic properties and MCE of $Gd_3NiSi_2$ alloy [33]. The maximal value of $-\Delta S_M$ is 3.6 J/kg K for annealed $Gd_3NiSi_2$ sample and 2.0 J/kg K for $Gd_3NiSi_2$ ribbon under a magnetic field change of 0–2 T at the Curie temperature $T_C$ = 215 K [33]. Although the value of $-\Delta S_M$ is not too large, $\Delta S_M - T$ curves of

* Corresponding author at: State Key Laboratory of Magnetism, Institute of Physics, Chinese Academy of Sciences, Beijing 100190, People's Republic of China.
*E-mail address:* shenbaogen@yeah.net (B. Shen).

https://doi.org/10.1016/j.jmmm.2020.166551
Received 6 October 2019; Received in revised form 3 January 2020; Accepted 1 February 2020
Available online 03 February 2020
0304-8853/ 

$Gd_3NiSi_2$ shows a wide shoulder, which is benefit to the improvement of $\Delta T_{width}$ and RC value. In addition, Morozkin et al. reported a ferromagnetic-like transition at 135 K and spin reorientation around 53 K in $Tb_3NiSi_2$ alloy [34]. According the result of neutron diffraction, four types of mixed ferromagnetic-antiferromagnetic order below 130 K, 82 K, 66 K and 53 K were certified in this alloy [34]. Those significant consequences indicate that the $R_3NiSi_2$ materials may have a considerable value of $\Delta S_M$ and a wide $\Delta T_{width}$. In this paper, $Tb_3NiSi_2$ and $Dy_3NiSi_2$ alloys were selected to study in detail. The phase component, crystalline structure, magnetic transition and magnetocaloric effect of those alloys were highly characterized. It was found that both samples undergo several magnetic transitions with increasing temperature and it gives rise to a large $\Delta T_{width}$ and RC value in the wide temperature.

## 2. Material and methods

The $R_3NiSi_2$ (R = Tb, Dy) ingots were synthesized by arc-melting method on a water-cooled copper crucible under protection of high-purity argon atmosphere. The starting materials (Tb, Dy, Ni and Si, purity above 99.9 wt%) were weighted in terms of the stoichiometric amount. The oxide layers on the crude metals were abolished before weighting for better purity. 2 wt% excessive rare-earth simple substance was added by considering the weight loss during the arc melting. The samples were turned and re-melted for several times to ensure homogeneity. Then, the as-obtained ingots were sealed in a quartz tube fulfilled with high-purity argon atmosphere and annealed at 1073 K for 1 month and quenched in liquid nitrogen finally.

The X-ray diffraction (XRD) measurements were performed by using a Rigaku SmartLab diffractometer with Cu $K_\alpha$ radiation ($\lambda$ = 1.541 Å), to analyze the phase component and the crystalline structure of the samples. A field-emission scanning electron microscope (FESEM, Hitachi S-4800) and an Oxford Instrument INCA X-ray energy dispersive spectrometer (EDS) were used for characterizing the morphology and the composition of samples respectively. Magnetic properties of samples were examined using a superconducting quantum interference device magnetometer (SQUID-VSM). Zero-field-cooled (ZFC) and field-cooled (FC) magnetization versus temperature (M-T) curves were recorded at temperatures from 5 K to 300 K under an applied field of 0.01 T. The magnetic hysteresis (M-H) loops were measured at different temperature in magnetic fields ranging from −7 T to 7 T.

## 3. Results and discussion

Fig. 1 exhibits the typical powder XRD patterns and Rietveld refined results of the $R_3NiSi_2$ (R = Tb, Dy) samples at room temperature. Most of diffraction peaks can be identified as $Gd_3NiSi_2$-type structure (space group: *Pnma*, JCPDS PDF # 72-0218) and tiny impurities are also found in the two samples. Base on the results of B-SEM and EDS, the average atomic ratio of $R_3NiSi_2$ alloy can be determined and given in Table 1. Rietveld refined results of two samples show that {$Tb_3NiSi_2$} alloy contains about 93.81% wt% $Tb_3NiSi_2$ (phase A, marked with red shown in the inset of Fig. 1(a), the same below) and 6.19 wt% $Tb_5Si_3$ (phase B, orange). {$Dy_3NiSi_2$} alloy contains about 91.17% wt% $Dy_3NiSi_2$ (phase C, red) and 8.83 wt% $Dy_5Si_3$ (phase E, orange). It should be noted that $Dy_{46}Ni_{23}Si_{31}$ (phase D, blue) cannot be added to Rietveld refined result due to the unknown crystal structure. The lattice parameters from the result of Rietveld refined are listed in Table 2. Compared with the literature [31–33], the lattice parameter values of *a*, *b* and *c* for two prepared samples are greatly close to the result reported in the literature [32] and decrease when R changes from element Sm to Dy due to the effect of lanthanide contraction, indicating that the results of Rietveld refined are reasonable.

Fig. 2(a) and (b) display the temperature dependence of the magnetization of $R_3NiSi_2$ (R = Tb, Dy) compounds under a magnetic field of 0.01 T, collected from 5 K to 300 K. The measurement process is

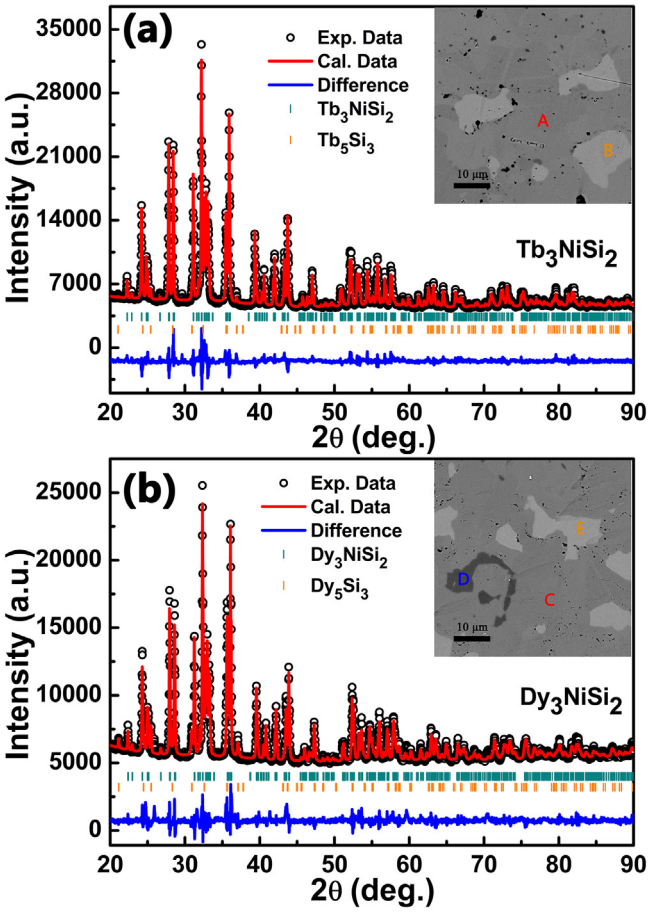


**Fig. 1.** XRD patterns and Rietveld refined results of (a) $Tb_3NiSi_2$ and (b) $Dy_3NiSi_2$ compounds measured at room temperature. The experiment data are indicated by hollow circles; the calculated profile is the continuous red line overlying them; the short vertical green and orange lines indicate the angular positions of the Bragg peaks of $R_3NiSi_2$ and $R_5Si_3$; the lower blue curve shows the difference between the observed and calculated intensity. The insets show the B-SEM images of two samples, respectively. (For interpretation of the references to color in this figure legend, the reader is referred to the web version of this article.)

**Table 1**
Atomic ratio of different phase for $R_3NiSi_2$ (R = Tb, Dy) compounds according to the results of B-SEM and EDS.

| Phase | Tb | Dy | Ni | Si |
|---|---|---|---|---|
| A ($Tb_3NiSi_2$) | 0.5196 | – | 0.1759 | 0.3045 |
| B ($Tb_5Si_3$) | 0.6499 | – | – | 0.3501 |
| C ($Dy_3NiSi_2$) | – | 0.5164 | 0.1850 | 0.2986 |
| D ($Dy_{46}Ni_{23}Si_{31}$) | – | 0.4590 | 0.2327 | 0.3083 |
| E ($Dy_5Si_3$) | – | 0.6635 | – | 0.3365 |

**Table 2**
Unit cell data of $Gd_3NiSi_2$-type $R_3NiSi_2$ (R = Sm, Gd, Tb and Dy) compounds (space group Pnma).

| Compound | a (nm) | b (nm) | c (nm) | Refs. |
|---|---|---|---|---|
| $Sm_3NiSi_2$ | 1.1505(3) | 0.4189(3) | 1.1383(3) | [29] |
| $Gd_3NiSi_2$ | 1.1398 | 0.4155 | 1.1310 | [28] |
| | 1.1410 | 0.4158 | 1.1322 | [30] |
| $Tb_3NiSi_2$ | 1.1306(2) | 0.4132(1) | 1.1212(3) | [29] |
| | 1.1313 | 0.4132 | 1.1222 | This work |
| $Dy_3NiSi_2$ | 1.1248(2) | 0.4119(1) | 1.1156(3) | [29] |
| | 1.1246 | 0.4118 | 1.1164 | This work |

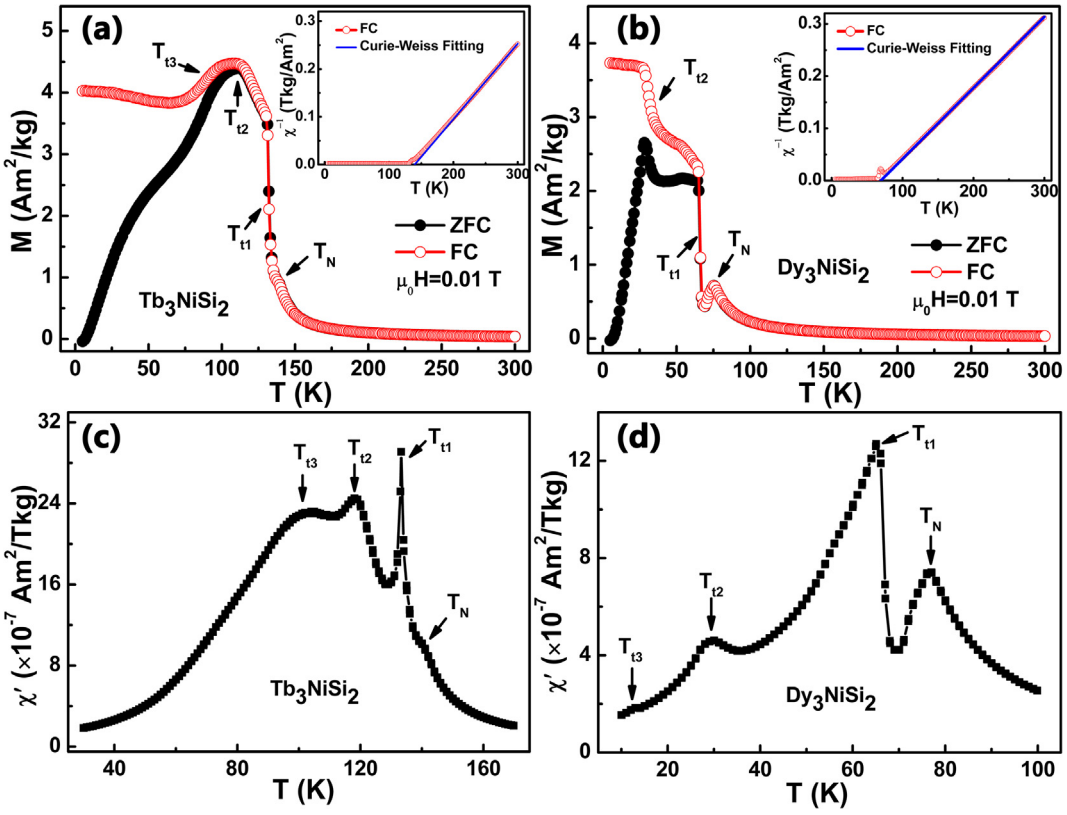


**Fig. 2.** Temperature dependences of ZFC and FC magnetization under a magnetic field of 0.01 T for (a) $Tb_3NiSi_2$, (b) $Dy_3NiSi_2$ samples. The inset shows the temperature dependence of reciprocal magnetic susceptibility $\chi^{-1}$. The temperature dependence of real part of AC magnetic susceptibility ($\chi' - T$) curve under the amplitude of 0.001 T and the frequency of 47 Hz of (c) $Tb_3NiSi_2$, (d) $Dy_3NiSi_2$ compounds.

performed in the zero-filed-cooled (ZFC) and field-cooled (FC) mode. As shown in Fig. 2(a), $Tb_3NiSi_2$ sample firstly undergoes a transition from antiferromagnetism (AFM) to ferromagnetism (FM) at 92 K ($T_{t3}$) with the increase of the temperature, and then a transition from FM to FM (spin reorientation) occurs at 114 K ($T_{t2}$). The magnetization decreases quickly when the temperature increases to 134 K ($T_{t1}$), indicating a transition from FM state to AFM state. At last, two tiny peaks at 140 K ($T_N$) both have been seen in the ZFC-FC curves with the decrease of the temperature, which manifests a transition from AFM to paramagnetism (PM) in $Tb_3NiSi_2$ sample. The inset of Fig. 2(a) shows the temperature dependence of reciprocal magnetic susceptibility $\chi^{-1}$. Curie-Weiss law is employed to analyze the data in the paramagnetic region, and a linear fit was obtained (160–300 K). The result shows that the paramagnetic Curie temperature $\theta_p$ is about 139.8 K and the effective magnetic moment ($\mu_{eff}$) per Tb atom is about 9.99 $\mu_B$, which is slightly larger than the theoretical value of 9.72 $\mu_B$ for $Tb^{3+}$ [35,36]. It can be concluded that the magnetism in $Tb_3NiSi_2$ compound mainly comes from the Tb atoms while Ni atoms are likely to be non-magnetic or very weak magnetic, which is similar to other rare-earth alloys [37–40].

The magnetization vs temperature of $Dy_3NiSi_2$ sample is depicted in Fig. 2(b), which is similar to $Tb_3NiSi_2$ sample. With the temperature increased, it undergoes a FM-to-FM transition (spin orientation) at about 30 K ($T_{t2}$). When the temperature rises to about 66 K ($T_{t1}$), a magnetic transition from FM to AFM state occurs and then it has a change of magnetism from AFM to PM when the temperature increases to 76 K ($T_N$). The paramagnetic Curie temperature ($\theta_p$) derived from the Curie-Weiss fitting is about 68.6 K and the effective magnetic moment ($\mu_{eff}$) per Dy atom is about 10.87 $\mu_B$, which is close to the theoretical value of 10.65 $\mu_B$ for $Dy^{3+}$ [35–37], indicating that Ni atoms have less contribution to the magnetism in $Dy_3NiSi_2$ sample.

To determine precisely the temperature of magnetic transitions, the temperature dependence of AC magnetic susceptibility curves for two samples are measured under the amplitude of 0.001 T and the frequency of 47 Hz in the temperature range from 10 K to 160 K for $Tb_3NiSi_2$ sample and 10 K to100 K for $Dy_3NiSi_2$ sample. For $Tb_3NiSi_2$ sample, as shown in Fig. 2(c), four cusps at 140.6 K, 134.2 K, 115 K and 94 K, are observed in the temperature dependence of real part of AC magnetic susceptibility ($\chi' - T$) curve, corresponding to four temperatures of magnetic transition in ZFC-FC M-T curves. It is noteworthy that some of four temperatures are not consistent with the previous literature. For example, $T_N$ cannot be reported for $Tb_3NiSi_2$ compound [34]. In addition, one can find that the broad shoulder instead of the obvious peak can be observed around $T_{t1}$. While as for $Dy_3NiSi_2$ sample (shown in Fig. 2(d)), one can also find four cusps at 76.6 K, 65.4 K, 29.3 K and 12.3 K in the $\chi' - T$ curve, which are agreement with three magnetic transition temperatures in ZFC-FC M-T curves. However, the magnetic transition temperature at 12.3 K cannot be distinctly found in ZFC-FC M-T curves. No references with respect to the magnetization of $Dy_3NiSi_2$ alloy have been reported yet, hence the magnetization of $Dy_3NiSi_2$ alloy needs to be studied it further. It should be mentioned that $Tb_5Si_3$ alloy is known to undergo two antiferromagnetic transitions at 72 K ($T_{N1}$) and 55 K ($T_{N2}$) [41], lower than magnetic transition temperatures detected in $\chi' - T$ curve of $Tb_3NiSi_2$ sample. At the same time, transition temperatures for $Dy_3NiSi_2$ sample are about at 150 K and 110.8 K [42], or 120 K and 84 K [43], higher than measured transition temperatures. As a result, it can be inferred reasonably that the impurities have less effect to magnetic measurement of two prepared samples.

The initial magnetization curves and the magnetic hysteresis loops at different temperatures are measured with applied fields up to 7 T, as shown in Figs. 3 and 4. Fig. 3(a) displays initial magnetization curve and the magnetic hysteresis loop at 5 K of $Tb_3NiSi_2$ sample. The inset of Fig. 3(a) shows the enlarged view of the hysteresis loop with magnetic field up to 0.1 T. In terms of the magnetization curve, the magnetization

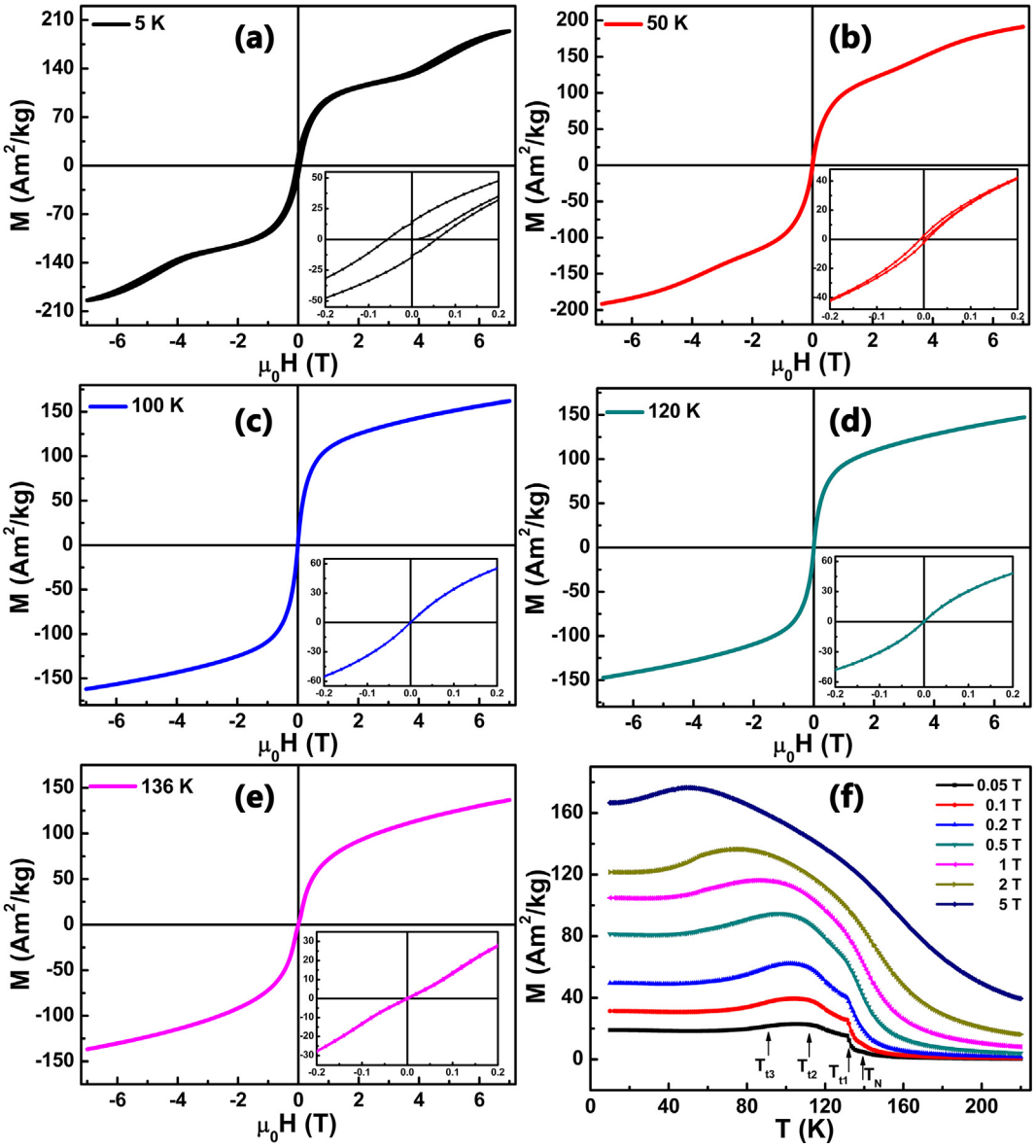


**Fig. 3.** M-H initial magnetization curves and hysteresis loops measured for $Tb_3NiSi_2$ compound at (a) 5 K, (b) 50 K, (c) 100 K, (d) 120 K and (e) 136 K. The inset displays the magnified view for every M-H curve. (f) Temperature dependences of magnetization under different magnetic fields for $Tb_3NiSi_2$ compound.

process divides clearly into two steps and a clear hysteresis exist in $Tb_3NiSi_2$ sample, which indicates the ground state of FM and AFM coexist in the sample. Consequently, it shows a field-induced metamagnetic transition from AFM to FM [44]. Moreover, according to the magnetic hysteresis loops at 50 K, 100 K, and 120 K (Fig. 3(c, d)), the hysteresis phenomenon gradually becomes weak and disappear with the increasing temperature. While for the magnetic hysteresis loop at 120 K between $T_{t1}$ and $T_{t2}$, one can obviously know that the sample presents a character of FM because the magnetization rises quickly as the magnetic field increases. However, the magnetic hysteresis loop at 136 K (Fig. 3(e)) between $T_N$ and $T_{t1}$ shows a linear magnetization process, indicating a character of AFM. The critical field is about 0.055 T and almost has no magnetic hysteresis. The magnetization does also not get saturation at this temperature when magnetic field lifts to 7 T, which may result from thermal disturbance to magnetic moment at high temperature. Fig. 3(f) shows M-T curves under different magnetic fields from 0.05 T to 5 T. It can be obviously seen that $T_{t3}$ corresponding to region of AFM-FM transition moves to lower temperature with increasing the applied magnetic field, also proving a behavior of metamagnetic transition between $T_{t2}$ and $T_{t3}$ [38], which is consistent with the analysis of M-H curves above.

Fig. 4 reveals the field dependence of the magnetization for $Dy_3NiSi_2$ sample. The rapidly increase of the magnetization at low magnetic field has been observed from the M-H curve at 5 K and the curve shows a large hysteresis effect. It has been normally thought as a typical feature of ferromagnetic ground state [38,39]. As for the M-H curves at 50 K (Fig. 4(b)) between $T_{t1}$ and $T_{t2}$, the magnetization rises sharply, but has almost no magnetic hysteresis effect. Moreover, the field dependence of the magnetization for $Dy_3NiSi_2$ sample at 70 K (Fig. 4(c)) between $T_N$ and $T_{t1}$ also exhibits a line behavior under the low-filed range between 0 and 0.08 T, which is similar with the M-H curve at 136 K of $Tb_3NiSi_2$ sample. However, no magnetic hysteresis effect happened at this temperature, which is beneficial to the application of magnetic refrigerant. Therefore, it can demonstrate that $Dy_3NiSi_2$ compound undergoes a PM-AFM transition at $T_N$, and an AFM-FM transition at $T_{t1}$.

Fig. 5 displays the isothermal magnetization curves (M-H curves) of $Tb_3NiSi_2$ sample. The data are measured using a ZFC mode under applied fields up to 7 T, in a temperature range from 8 K to 191 K. Aiming at determining the magnetic states at different temperatures, the M-H

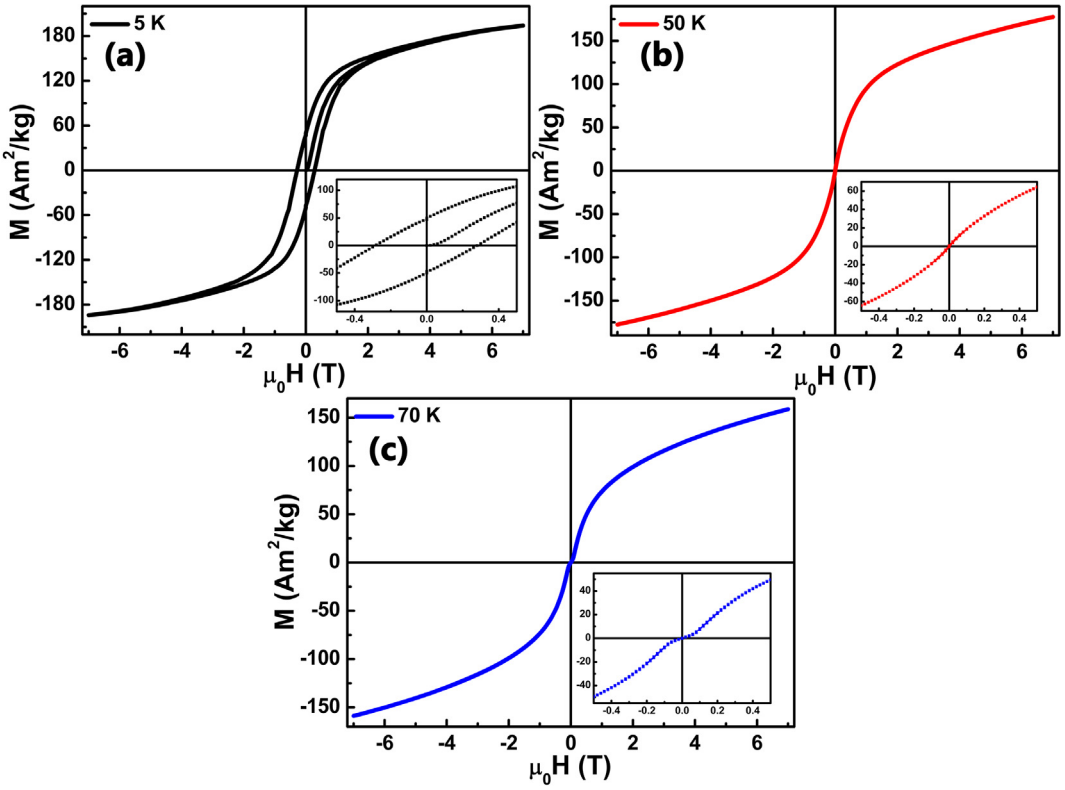


**Fig. 4.** M-H initial magnetization curves and hysteresis loops measured for $Dy_3NiSi_2$ compound at (a) 5 K, (b) 50 K and (c) 70 K. The inset displays the magnified view for every M-H curve.

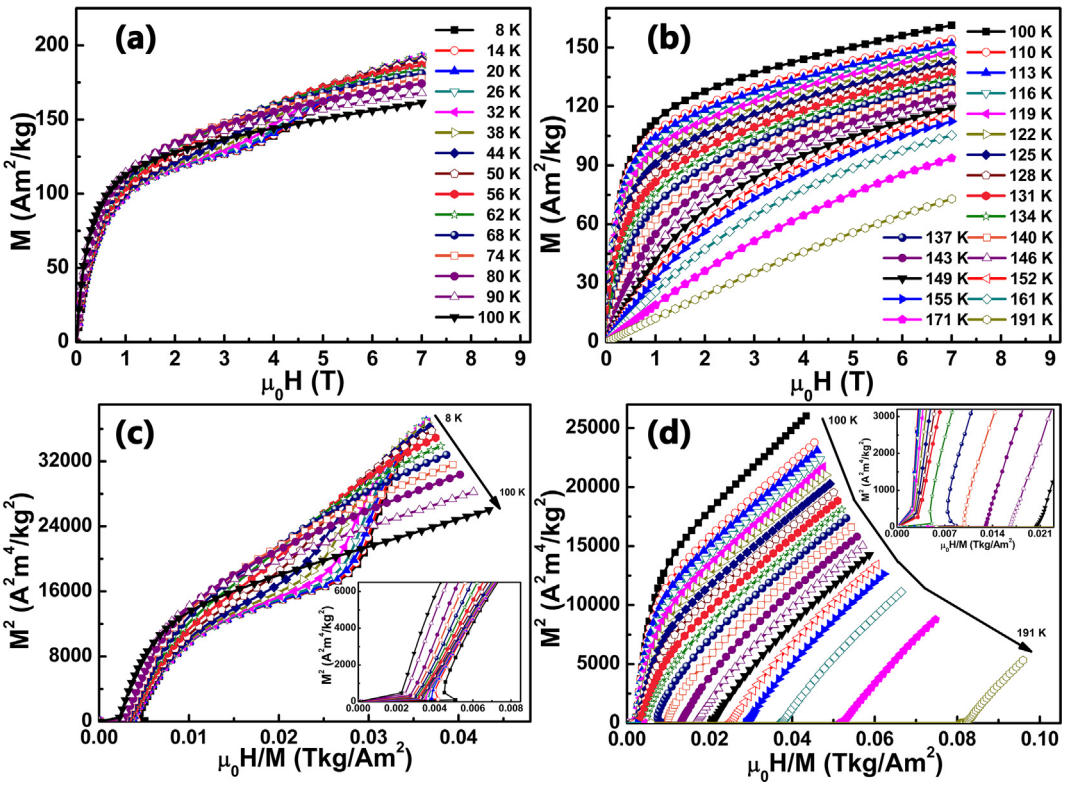


**Fig. 5.** Isothermal magnetization curves for $Tb_3NiSi_2$ compound at temperature from (a) 8 K–100 K, (b) 100 K–191 K. (c) Corresponding Arrott plots at temperature from (c) 8 K–100 K, (d) 100 K–191 K. The insets display the magnified view of corresponding Arrott plots.

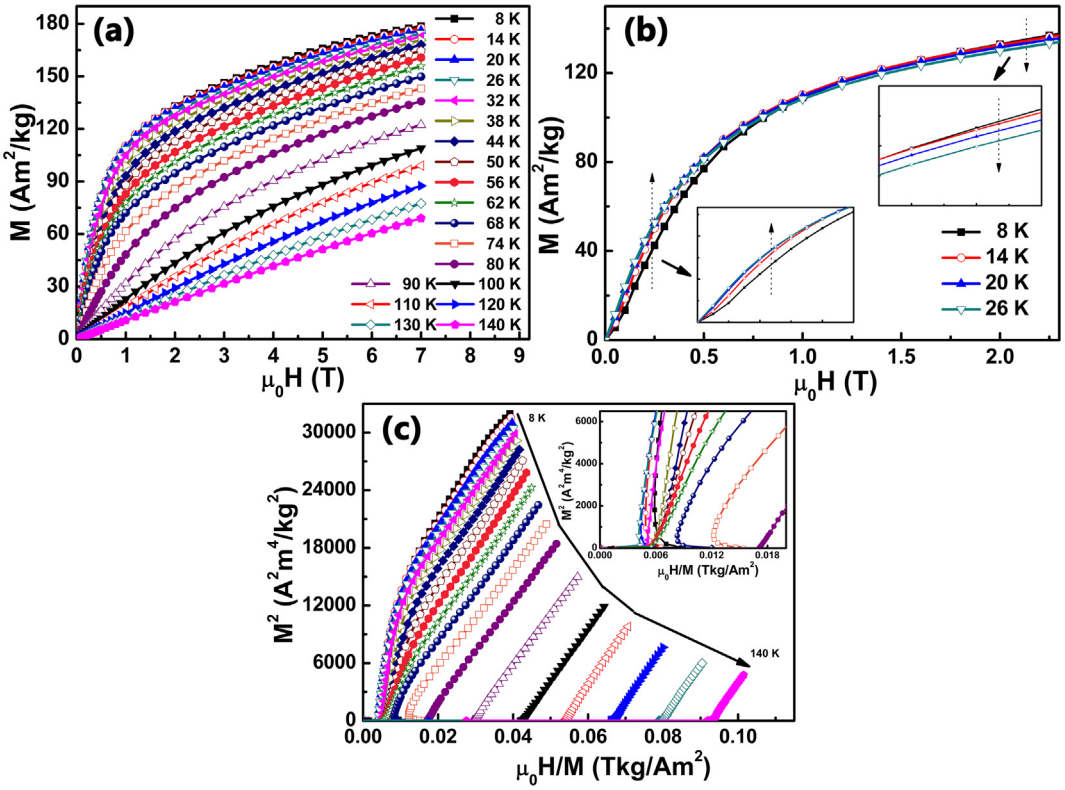


**Fig. 6.** (a) Isothermal magnetization curves for $Dy_3NiSi_2$ compound at 8 K–100 K. (b) M-H curves of $Dy_3NiSi_2$ compound at low fields from 8 K to 26 K. (c) Corresponding Arrott plots. The inset of (c) display the magnified view of corresponding Arrott plots.

curves are divided into two different temperature regime, i.e., 8 K–100 K (shown in Fig. 5(a)) and 100 K–191 K (shown in the Fig. 5(b)). Arrott-plots derived from $M^2 - \mu_0H/M$ relationship according to the M-H data are displayed in Fig. 5(c) and (d). In general, the magnetization value at 7 T decreases with increasing temperature. While for the Arrott plots between 8 K and100 K in Fig. 5(c), it can be seen that the Arrott curves have a small negative slope at 8 K and 14 K under the low field and presents an "S" shape under the high field, meaning the existence of first order magnetic transition [13]. Fig. 5(b) shows the initial magnetization curve between 100 K and 191 K. The magnetization saturates quickly at the lower field and then continues to increase with increasing the magnetic field, which shows ferromagnetic characteristics. In term of Arrott plots of Fig. 5(d), it can be clearly seen that the Arrott curves of 137 K and 140 K have a negative slope at the low field and behave the "S" shape, verifying further that the magnetic transition at $T_N$ is first-order phase transition as well [13].

Similar analysis is applied to $Dy_3NiSi_2$ sample. Fig. 6(a) shows the magnetic field vs magnetization curves at different temperatures, namely, from 8 K to 100 K. Fig. 6(b) shows the partial enlarged M-H curves of $Dy_3NiSi_2$ compound under low fields from 8 K to 26 K, respectively. The magnetization increases with increasing temperature under low magnetic field (below 0.86 T) while an opposite behavior presented under the higher magnetic field (above 0.86 T), which indicates that the ground state of the sample also exists weak AFM at low temperature [38,39]. However, it cannot be found from ZFC-FC M-T curves and the analysis of ground state on the basis of M-H curves at 5 K (Fig. 4(a)). The reason is that the signal could have been overlapped by FM signal in M-T curves measured at a magnetic field of 0.01 T. When the measuring method of AC magnetic susceptibility is employed, the AFM signal has not been masked entirely because the applied magnetic field (0.001 T) is smaller. Considering that a special transition temperature at 12.3 K is observed in AC magnetic susceptibility curve of $Dy_3NiSi_2$ sample (Fig. 2(d)), unknown $Dy_{46}Ni_{23}Si_{31}$ phase may contribute to this weak AFM ground state. Fig. 6(c) exhibits that the Arrott curves at 68 K and 74 K below $T_N$ have a small negative slope in the low field, which confirms $Dy_3NiSi_2$ is the first-order phase transition at $T_N$ as well as the above $Tb_3NiSi_2$ sample.

The isothermal magnetic entropy changes are normally calculated from the isothermal magnetization data by using Maxwell's relationship $\Delta S_M = \int_0^H \left(\frac{\partial M}{\partial T}\right)_H dT$, which is also used in this paper. The $\Delta S_M$ as a function of temperature ($\Delta S_M - T$ curves) under different magnetic field changes are shown in Fig. 7 for $Tb_3NiSi_2$ and $Dy_3NiSi_2$ compounds, respectively. As shown in Fig. 7(a) for $Tb_3NiSi_2$ compound, a valley and three peaks with increasing temperature from the curve (shown by the shot dot lines in the Fig. 7(a)), which corresponds four magnetic transition temperatures in the M-T curves. The valley of magnetic entropy change stands for inverse magnetocaloric effect ($\Delta S_M$ is positive value), which confirms antiferromagnetic exchange in $Tb_3NiSi_2$ compound at low temperature [40]. The maximum value of $\Delta S_M$ for $Tb_3NiSi_2$ compound is 2.3 J/kg K at 47 K under the magnetic field changes 0–7 T due to the filed-induced metamagnetic transition at $T_{t1}$ which makes AFM-FM transition move to lower temperature with increasing the applied magnetic field. On the other hand, three peaks are located just near the temperature of $T_{t2}$, $T_{t1}$ and $T_N$. The maximal value of $-\Delta S_M$ lies to the $T_N$, which demonstrates that magnetic transition at $T_N$ cannot result from the little purity in the $Tb_3NiSi_2$ sample. Hence it is further considered that $T_N$ is the temperature of AFM-PM transition of $Tb_3NiSi_2$ compound. On the basis of Fig. 7(a), the maximum value of $-\Delta S_M$ for $Tb_3NiSi_2$ compound are about 4.5 J/kg K and 11.1 J/kg K at 141 K ($T_N$) under the magnetic field changes of 0–2 T and 0–7 T, respectively. Analogously, it can be seen from Fig. 6(b) that the maximum values of $-\Delta S_M$ for $Dy_3NiSi_2$ sample are confirmed to be 3.6 J/kg K and 10.8 J/kg K at about 77 K for a field changes of 0–2 T and 0–7 T respectively, and also exhibits the peak around $T_N$. The RC value is estimated with the formula $RC = \int_{T1}^{T2} |\Delta S_M|\, dT$, where $T_1$ to $T_2$ stands for the temperature range of refrigeration. Generally speaking, peaks of magnetocaloric changes always emerge near the magnetic transition temperatures. Multiple transition temperatures generate multiple peaks, which can

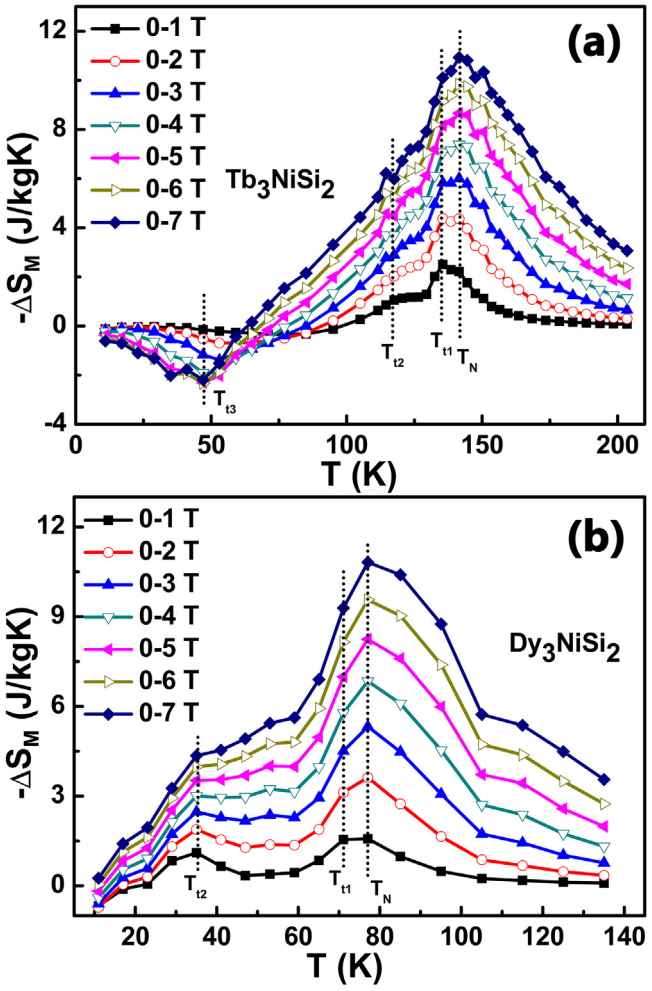


**Fig. 7.** Magnetic entropy changes $\Delta S_M$ as a function of temperature for (a) $Tb_3NiSi_2$, (b) $Dy_3NiSi_2$ compounds under the magnetic field changes of 0–1 T, 0–2 T, 0–3 T, 0–4 T, 0–5 T, 0–6 T and 0–7 T.

lead to the enhancement of $\Delta T_{width}$ and RC value. The temperature range of refrigeration $\Delta T_{width}$ and the value of RC are 66.9 K and 549.1 J/kg for $Tb_3NiSi_2$, and 64.0 K and 489.6 J/kg for $Dy_3NiSi_2$, respectively.

## 4. Conclusions

In conclusion, $R_3NiSi_2$ (R = Tb, Dy) samples with orthorhombic crystal structure were prepared by traditional arc-melting method. The results of B-SEM and EDS measurement reveal that $R_3NiSi_2$ samples contain mainly $R_3NiSi_2$ phase and $R_5Si_3$ phase. Besides, the $Dy_3NiSi_2$ sample exists small unknown $Dy_{46}Ni_{23}Si_{31}$ phase. Several magnetic transitions are found in both $R_3NiSi_2$ compounds and magnetocaloric effect was investigated in detail, finding that the maximal value of MCE are about 4.5 J/kg K and 11.1 J/kg K at 141 K for $Tb_3NiSi_2$ compound under a field change of 0–2 T and 0–7 T respectively, while the maximal value of MCE are about 3.6 J/kg K and 10.8 J/kg K at 77 K for a field change of 0–2 T and 0–7 T respectively for $Dy_3NiSi_2$ compound. The large value of $\Delta T_{width}$ and RC are 66.9 K and 549.1 J/kg for $Tb_3NiSi_2$ compound, and 64.0 K and 489.6 J/kg for $Dy_3NiSi_2$ compound due to several magnetic transitions. In view of the common character of rare-earth elements, it may be feasible to adjust to the refrigeration temperature range by the substitution of different rare-earth elements in $R_3NiSi_2$-family compounds.

## Author statement

Baogen Shen and Zhiyi Xu conceived and designed the experiments. Jun Liu synthesized the samples. Yan Zhang and Dan Liu contributed to X-ray diffraction measurements and Rietveld refined results. Xinqi Zheng and Lichen Wang contributed to magnetization measurements. Jiawang Xu, Xinqi Zheng, Jirong Sun and Fengxia Hu contributed to the result analysis. Jun Liu, Shulan Zuo, Baogen Shen and Tongyun Zhao analyzed the data and wrote the manuscript. All authors discussed the results and commented on the manuscript.

## Declaration of Competing Interest

The authors declare that they have no known competing financial interests or personal relationships that could have appeared to influence the work reported in this paper.

## Acknowledgements

This work was supported by the National Key Research and Development Program of China (Grant No. 2016YFA0300701, 2016YFB0700903), the National Natural Science Foundation of China (Grant No. 51590880, 11520101002) and the Key Program of the Chinese Academy of Sciences of China (Grant No. KJZD-EW-M05-1, KJZD-EW-M05-3, QYZDY-SSW-SLH020, 112111KYSB20180013).

## References

[1] A.M. Tishin, Magnetocaloric Effect in the Vicinity of Phase Transitions, vol. 12, North-Holland, Amsterdam, 1999, p. 398.
[2] G.V. Brown, Magnetic heat pumping near room temperature, J. Appl. Phys. 47 (1976) 3673–3680.
[3] K.A. Gschneidner Jr., V.K. Pecharsky, A.O. Tsokol, Recent developments in magnetocaloric materials, Rep. Prog. Phys. 68 (2005) 1479–1539.
[4] B.G. Shen, J.R. Sun, F.X. Hu, H.W. Zhang, Z.H. Cheng, Recent progress in exploring magnetocaloric materials, Adv. Mater. 21 (2009) 4545–4564.
[5] X.Q. Zheng, B.G. Shen, The magnetic properties and magnetocaloric effect in binary R-T (R = Pr, Gd, Tb, Dy, Ho, Er, Tm; T = Ga, Ni Co, Cu) intermetallic compounds, Chin. Phys. B 26 (2017) 027501.
[6] W.F. Giauque, D.P. Macdougall, Attainment of temperature below 1° absolute by demagnetization of $Gd_2(SO_4)_3{\cdot}8H_2O$, Phys. Rev. B 43 (1933) 768.
[7] J.A. Barclay, W.A. Steyert, Materials for magnetic refrigeration between 2 K and 20 K, Cryogenics 22 (1982) 73–80.
[8] R.D. Shull, Magnetocaloric effect of ferromagnetic particles, IEEE Trans. Magn. 29 (1993) 2614.
[9] R.D. McMichael, J.J. Ritter, R.D. Shull, Enhanced magnetocaloric effect in $Gd_3Ga_{5-x}FexO_{12}$, J. Appl. Phys. 73 (1993) 6946.
[10] H. Zhang, Y.J. Sun, E. Niu, L.H. Yang, J. Shen, F.X. Hu, J.R. Sun, B.G. Shen, Large magnetocaloric effects of RFeSi (R = Tb and Dy) compounds for magnetic refrigeration in nitrogen and natural gas liquefaction, Appl. Phys. Lett. 103 (2013) 202412.
[11] H. Zhang, B.G. Shen, Z.Y. Xu, J. Shen, F.X. Hu, J.R. Sun, Y. Long, Large reversible magnetocaloric effects in ErFeSi compound under low magnetic field change around liquid hydrogen temperature, Appl. Phys. Lett. 102 (2013) 092401.
[12] Y. Zhang, Q.Y. Dong, L.C. Wang, M. Zhang, H.T. Yan, J.R. Sun, F.X. Hu, B.G. Shen, Giant low-field reversible magnetocaloric effect in HoCoGe compound, RSC Adv. 6 (2016) 106171.
[13] L.C. Wang, Q.Y. Dong, J. Lu, X.P. Shao, Z.J. Mo, Z.Y. Xu, J.R. Sun, F.X. Hu, B.G. Shen, Low-temperature large magnetocaloric effect in the antiferromagnetic CeSi compound, J. Alloys Compd. 587 (2014) 10–13.
[14] S.M. Benford, G.V. Brown, T-S diagram for gadolinium near the Curie temperature, J. Appl. Phys. 52 (1981) 2110.
[15] B.K. Ponomarev, Magnetic properties of gadolinium in the region of paraprocess, J. Magn. Magn. Mater. 61 (1986) 129–138.
[16] V.K. Pecharsky, K.A. Gschneidner Jr., Giant magnetocaloric effect in $Gd_5(Si_2Ge_2)$, Phys. Rev. Lett. 78 (1997) 4494–4497.
[17] V.K. Pecharsky, G.D. Samolyuk, V.P. Antropov, A.O. Pecharsky, K.A. Gschneidner, Jr., The effect of varying the crystal structure on the magnetism, electronic structure and thermodynamics in the $Gd_5(Si_xGe_{1-x})_4$ system near x = 0.5, J. Solid State Chem. 171 (2003) 57–68.
[18] J.M. Wu, F. Li, L.Y. Cui, L.C. Tai, The magnetic entropy change properties of $La_{1-z}R_z(Fe_{1-x-y}Co_xAl_y)_{13}$, Compounds 79 (1996) 982.
[19] F.X. Hu, B.G. Shen, J.R. Sun, Z.H. Cheng, G.H. Rao, X.X. Zhang, Influence of negative lattice expansion and metamagnetic transition on magnetic entropy change in the compound $LaFe_{11.4}Si_{1.6}$, Appl. Phys. Lett. 78 (2001) 3675.
[20] A. Fujita, K. Fukamichi, J.-T. Wang, Y. Kawazoe, Large magnetovolume effects and band structure of itinerant-electron metamagnetic $La(Fe_xSi_{1-x})_{13}$ compounds, Phys.

Rev. B 68 (2003) 104431.
[21] F.X. Hu, B.G. Shen, J.R. Sun, G.J. Wang, Z.H. Cheng, Very large magnetic entropy change near room temperature in $LaFe_{11.2}Co_{0.7}Si_{1.1}$, Appl. Phys. Lett. 80 (2002) 826.
[22] B.G. Shen, F.X. Hu, Q.Y. Dong, J.R. Sun, Magnetic properties and magnetocaloric effects in $NaZn_{13}$-type La(Fe, Al)$_{13}$-based compounds, Chin. Phys. B 22 (2013) 017502.
[23] N.K. Singh, K.G. Suresh, A.K. Nigam, S.K. Malik, A.A. Coelho, S. Gama, Itinerant electron metamagnetism and magnetocaloric effect in $RCo_2$-based Laves phase compounds, J. Magn. Magn. Mater. 317 (2007) 68–79.
[24] J. Ćwik, Experimental study of the magnetocaloric effect in $Dy_{1-x}Er_xCo_2$ solid solutions doped with Gd, J. Alloys Compd. 580 (2013) 341–347.
[25] J. Ćwik, Magnetism and magnetocaloric effect in multicomponent Laves-phase compounds: study and comparative analysis, J. Solid State Chem. 209 (2014) 13–22.
[26] J. Shen, J.L. Zhao, F.X. Hu, G.H. Rao, G.Y. Liu, J.F. Wu, Y.X. Li, J.R. Sun, B.G. Shen, Magnetocaloric effect in antiferromagnetic $Dy_3Co$ compound, Appl. Phys. A 99 (2010) 853–858.
[27] H. Zhang, Z.Y. Xu, X.Q. Zheng, J. Shen, F.X. Hu, J.R. Sun, B.G. Shen, Giant magnetic refrigerant capacity in $Ho_3Al_2$ compound, Solid State Commun. 152 (2012) 1127–1130.
[28] Q.Y. Dong, J. Chen, J. Shen, J.R. Sun, B.G. Shen, Magnetic properties and magnetocaloric effects in $R_3Ni_2$ (R = Ho and Er) compounds, Appl. Phys. Lett. 99 (2011) 132504.
[29] S.K. Dhar, P.L. Paulose, A. Palenzona, P. Manfrinetti, R. Cimberle, Multiple magnetic transitions in $R_3CoGe_2$ compounds (R = Ce, Pr and Nd), J. Magn. Magn. Mater. 270 (2004) 43–50.
[30] P. Manfrinetti, A.V. Morozkin, O. Isnard, F. Wrubl, Yu. Mozharivskyj, V. Svitlyk, Magnetic ordering of novel $La_3NiGe_2$-type $R_3CoGe_2$ compounds (R = Pr, Nd, Sm, Gd-Dy), Intermetallics 19 (2011) 321–326.
[31] K. Klepp, E. Parthé, Orthorhombic gadolinium nickel silicide $Gd_3NiSi_2$ with a Filled-up $Hf_3P_2$ structure type, Acta Crystallogr. 37 (1981) 1500–1504.
[32] K. Klepp, E. Parthé, $Sm_3NiSi_2$, $Tb_3NiSi_2$ and $Dy_3NiSi_2$ with the $Gd_3NiSi_2$ structure type, J. Less-Common Met. 83 (1982) L33–L35.
[33] S. Tencé, S. Gorsse, E. Gaudin, B. Chevalier, Magnetocaloric effect in the ternary silicide $Gd_3NiSi_2$, Intermetallics 17 (2009) 115–119.
[34] A.V. Morozkin, V. Svitlyk, Y. Mozharivskyj, O. Isnard, Magnetic order of the $La_3NiGe_2$-type $Tb_3NiSi_2$, J. Magn. Magn. Mater. 349 (2014) 201–207.
[35] S. Legvold, Rare earth metals and alloys, in: E.P. Wohlfarth (Ed.), Ferromagnetic Materials, North-Holland, Amsterdam, 1980, pp. 183–295.
[36] A.V. Morozkin, V.O. Yapaskurt, R. Nirmala, S.K. Malik, S. Quezado, J.L. Yao, Y. Mozharivskyj, A.K. Nigam, O. Isnard, Magnetic order of $Y_3NiSi_3$-type $R_3NiSi_3$ (R = Gd-DY) compounds, J. Magn. Magn. Mater. 398 (2016) 141–147.
[37] H. Zhang, Y.W. Li, E.K. Liu, Y.J. Ke, J.L. Jin, Y. Long, B.G. Shen, Giant rotating magnetocaloric effect induced by highly texturing in polycrystalline DyNiSi compound, Sci. Rep. 5 (2015) 11929.
[38] X.Q. Zheng, X.P. Shao, J. Chen, Z.Y. Xu, F.X. Hu, J.R. Sun, B.G. Shen, Giant magnetocaloric effect in $Ho_{12}Co_7$ compound, Appl. Phys. Lett. 102 (2013) 022421.
[39] X.Q. Zheng, B. Zhang, Y.Q. Li, H. Wu, H. Zhang, J.Y. Zhang, S.G. Wang, Q.Z. Huang, B.G. Shen, Large magnetocaloric effect in $Er_{12}Co_7$ compound and the enhancement of $\delta T_{FWHM}$ by Ho-substitution, J. Alloys Compd. 680 (2016) 617–622.
[40] X.Q. Zheng, Z.Y. Xu, B. Zhang, F.X. Hu, B.G. Shen, The normal and inverse magnetocaloric effect in $RCu_2$ (R = Tb, Dy, Ho, Er) compounds, J. Magn. Magn. Mater. 421 (2017) 448–452.
[41] A.V. Morozkin, O. Isnard, R. Nirmala, S.K. Malik, Magnetic properties and magnetic structure of the $Mn_5Si_3$-type $Tb_5Si_3$ compound, J. Alloys Compd. 470 (2009) 20–23.
[42] J.P. Semitelou, J.K. Yakinthos, The conical magnetic structure of $Dy_5Si_3$, J. Magn. Magn. Mater. 265 (2003) 152–155.
[43] J. Roger, M.B. Yahia, V. Babizhetskyy, J. Bauer, S. Cordier, R. Guérin, K. Hiebl, X. Rocquefelte, J.Y. Saillard, J.F. Halet, $Mn_5Si_3$-type host-interstitial boron rare-earth metal silicide compounds $RE_5Si_3$: crystal structures, physical properties and theoretical considerations, J. Solid State Chem. 179 (2006) 2310–2328.
[44] S.K. Dhar, P.L. Paulose, A. Palenzona, P. Manfrinetti, R. Cimberle, Multiple magnetic transitions in $R_3CoGe_2$ compounds, J. Magn. Magn. Mater. 270 (2004) 43–50.